An Efficient Rotationally Symmetric Approach for the Design of Sparse Conformal Arrays in Wide Angle Scanning

Pengfei Gu[*], Zhenhong Fan, Dazhi Ding, and Rushan Chen

Department of Communication Engineering, Nanjing University of Science and Technology, Nanjing, China
*pengfeigu@njust.edu.cn

Abstract ─ This paper addresses a novel rotationally symmetric technique with multiple constraints for sparse conformal array synthesis. The purpose is to synthesis a sparse optimal common element positions on the conformal surface varying multiple patterns of wide angle scanning with the behavior of low sidelobe levels (SLL). The conformal surface aperture is partitioned into several rotationally symmetric sections. The element positions and element numbers of only one section need to be optimized, which contribute to the reduction of optimizing variables and computation resources. We formulate the synthesis problem as a constrained optimization problem, which takes the peak sidelobe level (PSLL) as the fitness function, and sets the total number of array elements, the minimum spacing between two adjacent elements to form multiple constraints. The Brain Storm Optimization (BSO) is further exploited into the synthesis problem with multiple constraints. A set of representative numerical examples are presented to assess the advantages and effectiveness of the proposed method.

Index Terms ─ Conformal sparse array, rotational symmetry, wide angle scanning.

I. INTRODUCTION

Differ from the synthesis of sparse planar arrays, conformal antenna arrays show unparalleled advantages of reduced aerodynamic drag, saved space, and wide-angle coverage for applications in aircraft, missiles, naval ships and high-speed vehicles. With the wide application of array antennas in radar communication and electronic system, the number of array elements and corresponding complexity increase greatly, which cause great challenges to the limited platform space, the weight and cost of conformal array antennas.

Many stochastic optimization methods have been presented for the synthesis of sparse linear and planar arrays, such as genetic algorithm (GA) [1], [2], differential evolution (DE) [3], [4] algorithm, Particle swarm optimization (PSO) algorithm [5]. Recently, a series of synthesis techniques based on the sparse signal recovery theory of Bayesian compressive sampling (BCS) method [6], [7] and non-iterative approach named matrix pencil method (MPM) [8]-[10] are presented for the reconstruction of sparse arrays with desired pattern synthesis. Despite its success and efficiency, there are still many challenges for the synthesis and optimization of conformal sparse arrays. The inherent nonlinearity and non-planar directional anisotropy of conformal carrier surface lead to the inadaptability of the direct array pattern multiplication in the synthesis process. Most linear or planar array synthesis methods cannot be directly applied to the design of sparse conformal arrays.

Recently, many techniques of GA [11], [12], PSO [13]-[15], DE [16] and others [17], [18] have been extended to the synthesis of sparse conformal arrays. However, a relatively new global optimization method: Brain Storm Optimization (BSO), hasn't yet been applied in antenna and electromagnetic applications. Brain Storm Optimization (BSO), which was developed in 2011 by Shi, is a swarm intelligence optimization algorithm inspired by the collective behaviour of human beings in solving problems [19]. The application of BSO in different fields has shown to be successful [20]-[23]. But there is relatively few correlational research work for the design of sparse conformal arrays. To above stochastic or global optimization methods, they may fall into local optima and turn out to be relatively time-consuming when optimizing large arrays with various variables of positions, excitations and even the number of elements. Moreover, it may only fit for the sparse synthesis of one fixed or shaped-beam pattern. When applied to the case of reconfigurable multiple-patterns, it also has the problem that cannot guarantee the same best distribution varying multiple-patterns in wide-angle scanning. It is a technical difficulty and challenge to realize fast optimization of sparse conformal arrays, which considers the influence of conformal carrier-surface shape and element distribution on array behavior in wide angle scanning. How to effectively reduce the number of optimization variables is much more important.

Conformal array antennas are usually mounted onto a cylindrical, spherical, conical, or some other smoothly curved surfaces due to aerodynamic or hydrodynamic requirements [24], [25]. The characteristic of rotational

symmetry can be also found in the carrier such as the hemisphere, cylindrical, the cone and so on. The rotational symmetry characteristic [26] was firstly exploited into the optimization of thinned wideband planar arrays with the reduction of computational complexity and suppression of peak sidelobe level (PSLL). But it hasn't been found there are some researches of rotational symmetry technique for the optimization of large sparse conformal arrays.

   In the study, an effective and general approach is developed for the fast synthesis of sparse conformal array capable of radiating desired patterns varying scanning angles. The rotationally symmetry technique is exploited to accelerate the sparse conformal array synthesis process with the reduction of optimization variable number and computational complexity. The BSO algorithm is utilized to further improve radiation performance in wide-angle scanning by optimizing array element distributions. The constraint on the minimum element spacing and multiple-pattern performance is made to ensure finding the common best sparse element positions.

   The framework of the paper is organized in the following manner. In Section II, the problem formulation and the theory of the synthesis of sparse conformal arrays is presented. Numerical examples of sparse conformal array optimization demonstrate the validity of the proposed method in Section III. Finally, Section IV concludes the paper.

II. THEORY AND FORMULATION

A. Conformal array model

   Consider a conformal array of N elements located arbitrarily on a carrier surface as shown in Fig. 1, the total far field $F(\theta,\phi)$ of conformal phased arrays along the direction (θ,ϕ) in the global coordinate system can be expressed as below:

$$F^i(\theta,\phi) = \sum_{n=1}^{N} \omega_n^i E_n(\theta,\phi)\exp(jk\mathbf{r}_n\mathbf{u}),\qquad(1)$$

where $k = 2\pi/\lambda$ denotes the wave number, N is the total array element number. ω_n^i represents the complex excitation coefficient of the ith direction for the nth element, $\mathbf{r}_n = (x_n, y_n, z_n)$ is the location vector in the global coordinate system and $E_n(\theta,\phi)$ represents the nth vector pattern along the wave propagation direction $\mathbf{u}$. $\mathbf{u} = [\sin\theta\cos\phi, \sin\theta\sin\phi, \cos\theta]^T$ is the unit vector in the spherical coordinate system.

   Since each element on the carrier surface has its own position and orientation, it is more convenient to first consider the field of each element in their own coordinate system and then transform the field back to the global coordinate system. The coordinate transformation is exploited to superimpose all elements'

components at the far field $F(\theta,\phi)$ in the global coordinate system (x, y, z):

$$F(\theta,\phi) = \sum_{n=1}^{N} \omega_n Z_n^T E_n'(\theta_n',\phi_n')\exp(jk\mathbf{r}_n\mathbf{u}),\qquad(2)$$

where Z_n^T is the transform matrix form the local coordinate system of the nth element to the global coordinate system, and $E_n'(\theta_n',\phi_n')$ represents the vector pattern in the local coordinate system. More details can be referred to [12] and [18].
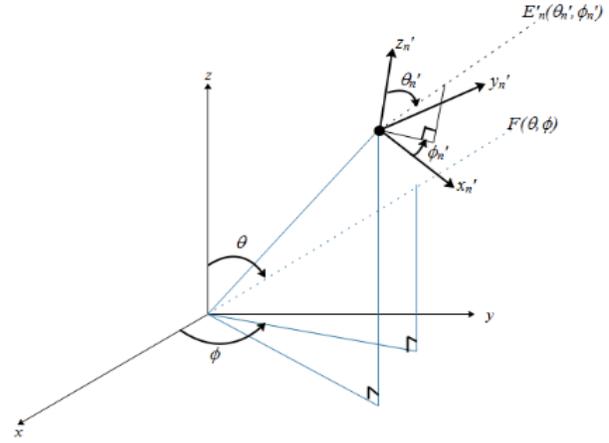

Fig. 1. Global and local coordinate system.

B. The synthesis procedure of sparse conformal array

   In the paper, we aim to design an effective synthesis method to redesign an optimal array distribution of sparse conformal array while maintaining the performance of desired low SLL and a constraint on the minimum element spacing of avoiding adjacent elements too close, which further avoids the intersection of two actual array units. Moreover, the sparse distribution of array elements and minimum element-spacing constraint contribute to larger spacing between units than that of uniform array, which slightly reduces the mutual coupling of array elements. The multi-objective optimizing model can be formed as:

$$\begin{cases} SLL = \max\left((F^i(\theta,\phi) \notin Mainbeam),\quad i=1,\cdots,T \right. \\ \Delta r_{mn} \geq d_{target},\quad m,n \in [1,N] \text{ and } m \neq n \end{cases},\qquad(3)$$

where SLL represents the maximum sidelobe level of the total array pattern $F(\theta,\phi)$ and Δr_{mn} is the distance of the mth and n^{th} array element. To avoid too close condition of adjacent elements, the minimum target element spacing of d_{target} is taken into account of the sparse conformal array optimizing procedure.

   Benefit from the conformal rotational symmetric technique, the element positions in only one-partitioned region is required to be optimized by the proposed synthesis method, which contributes to the effectively

reduction of optimization variables and computation complexity on large conformal arrays. The detailed introduction of 8-part truncated cone conformal array is illustrated in Fig. 2, where the rotational symmetric is partitioned into the whole structure with 8 parts ($\Delta\phi = 2\pi / Q = 2\pi / 8$). Two optimizable variables of ($r \leq r_q \leq R$, $0 \leq \phi_q \leq \Delta\phi$) are extracted from the geometry configuration, where r_q represents the radius of the truncated cone conformal surface and ϕ_q is the angle coverage of per-sector region. The coordinate of array elements along the z-sub coordinate can be got as below:

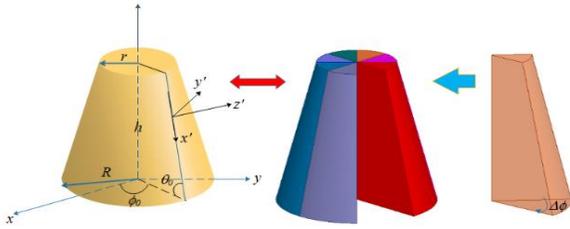$$z_q = \frac{R - r_q}{R - r} \cdot h . \qquad (4)$$

Fig. 2. Detailed division of truncated conformal array with 8 rotational symmetric parts.

The element position (x_q, y_q, z_q) can be easily got by the way above. It also fits for the cone conformal array. But for the hemisphere conformal array in Fig. 3, each array element distribution in the pie-shaped wedge can be simplistically expressed as two optimizable variables of ($r_q = R$, $0 \leq \phi_q \leq \Delta\phi$, $0 \leq \theta_q \leq \pi/2$). Depending on the characteristic of conformal rotational symmetry and proposed hybrid BSO wide-angle scanning multiple-pattern synthesis method, the extension to the effective synthesis of large or ultra-large scale sparse conformal arrays becomes feasible with the reduction of optimization variable number and computation complexity to some degree.
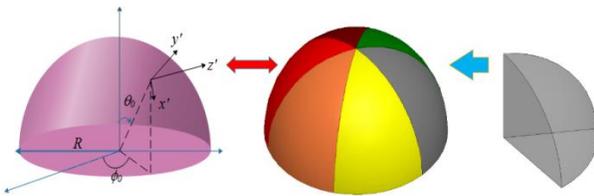

Fig. 3. Geometry of the rotationally symmetric hemisphere conformal array.

To ensure the constraint of minimum element spacing d_{target}, limits on the interval scope of r_q and ϕ_q for each array element location in the pie-shaped optimized slice are firstly considered. Meanwhile, the

neighbored elements in the neighbored slice are also considered to avoid placing two elements too close together. The planform of array elements on the rotational symmetrical carrier surface is shown as Fig. 4.
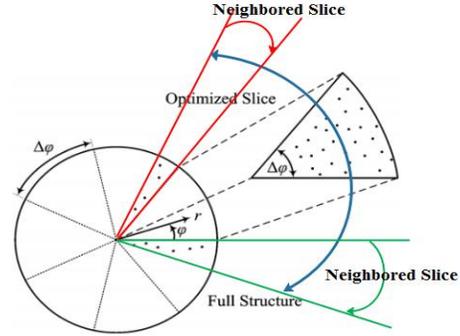

Fig. 4. Consideration of element spacing.

By using the constraints of minimum number of array elements, the minimum spacing between two adjacent elements and the optimizable SLLl in wide-angle scanning, the fitness function can be formulated as below:

$$f_{fit} = a \left| \left[\max(SLL_t) - PSLL \right] \right| + b \left| (d_{target} - \min(d_{target}, d_{min})) \right|, \quad t = 1, \cdots, T ,$$
$$(5)$$

where SLL_t ($t = 1, \cdots, T$) is the actual maximum sidelobe level of the tth pattern for the conformal sparse array in wide-angle scanning and $PSLL$ represents the desired minimum sidelobe level. The constraint on the synthesis of sparse conformal array varying multiple-patterns is addressed by the proposed method. d_{min} is the minimum element spacing of the optimized sparse conformal array. A criterion is built by the fitness function of Eq. (5), which aims at constraining on the minimum spacing d_{min} among conformal array elements and suppressing the SLL of multiple patterns to the desired index.

For the design and optimization of sparse conformal arrays, the variable parameters of r_q and ϕ_q ($q = 1, \cdots, N_Q$) for each element can be generated by the BSO method in each population and updated generation. The entire sparse conformal array is reconstructed by symmetrically rotating optimized conformal array element position in one part of Q-folds. The multi-objective optimizing model of Eq. (3) and fitness function of Eq. (5) is incorporated into a hybrid reformulation as:

$$\begin{cases} \min\left(N_Q\right) \\ SLL = \max\left((F^i(\theta, \phi) \notin Mainbeam), \quad i = 1, \cdots, T \right), \\ \Delta r_{mn} \geq d_{target}, \quad 1 \leq m, n \leq N, \ m \neq n, N = N_Q \cdot Q \end{cases} \quad (6)$$

where N_Q represents the element number of pie-optimized slice. SLL is a relatively worst extraction from the performance of maximum SLL within multiple-patterns in wide-angle coverage. The BSO is exploited

to optimize conformal designs to obtain deferent performance characteristics of conformal array far-field radiation patterns with fewer elements. It improves the probability of finding a solution by organizing ideas generated from a diverse group of individuals in the brainstorming process. It mainly contains three operations and a typical brainstorming process with optimizing steps is given as Fig. 5. For more information of BSO, the reader can refer to the reference [23].
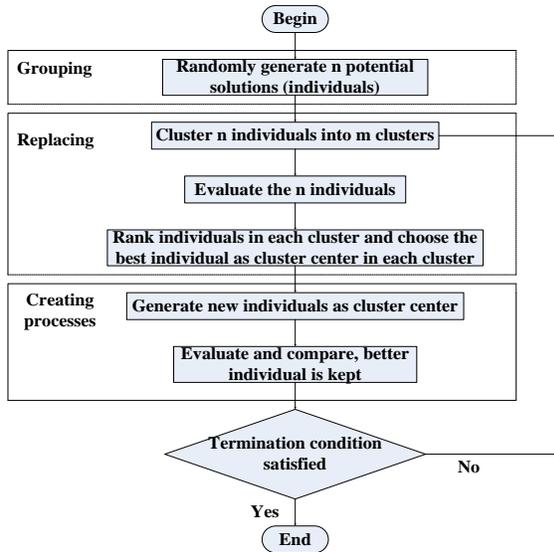
Fig. 5. Flowchart of the BSO algorithm.

The sparse ratio [9], [10] is defined as γ to account for the element saving of sparse conformal array compared with original conformal array:

$$\gamma = \frac{N - N'}{N} \times 100\% , \tag{7}$$

where N' is the number of optimized sparse conformal array antenna elements and N is the number of the original conformal uniform array element number with half-wavelength interval.

III. NUMERICAL RESULTS

In order to evaluate the efficiency and performance of the proposed method, several representative examples are studied for the synthesis of sparse conformal arrays in the section. All of synthesis examples are executed on a Sugon computing server of Intel Purley X745-G30 with 2TB RAM. d_{target} of all numerical examples are set as 0.5λ.

As the first synthesis examples, an effective design of a sparse hemisphere conformal array is presented by the proposed method. The initial $\lambda/2$ uniform spacing conformal array is composed of 7 circular ring sub-arrays distributed on the hemisphere carrier surface with 118 elements in all, see Fig. 6.
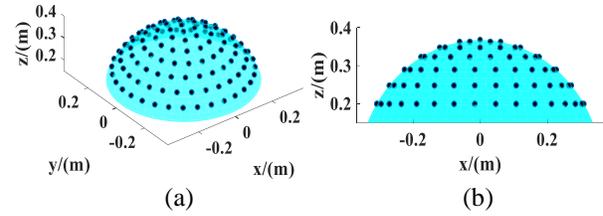

Fig. 6. (a) Uniform hemisphere array. (b) Left view of uniform hemisphere array.

The radius of the hemisphere is 3λ corresponding to the free wavelength at 2.45GHz. All elements are given uniform excitations. The hemisphere geometry is rotationally partitioned into 6 symmetric conformal regions. The optimized synthesis per region is designed to have N_Q array elements with $2N_Q$ optimizable variables, whose element of one symmetric part is restricted on the carrier surface region of ($r_q = 3\lambda$, $0 \le \phi_q \le 2\pi/6$, $0 \le \theta_q \le \pi/2$). The topmost unit remains motionless. The desired SLL is set as -25dB and iterative optimizing steps is set as 500 to ensure full convergence. d_{target} is 0.5λ. The design objective is to realize low SLL with fewer elements by only optimizing array distribution without excitations. Eventually, the optimized conformal sparse array reaches SLL of -25.45dB with a minimum element spacing of 0.51λ. The optimization time is 0.32 hour. The total element number of optimized array is 91 with sparse ratio γ of 23%. The optimized conformal sparse element locations are shown in Fig. 7 (a) and its top view is given in Fig. 7 (b). The array factor of optimized sparse conformal array is shown in Fig. 8 (a). The cut plane ϕ=26° of optimized sparse conformal array has the peak SLL of -25.45dB as in Fig. 8 (b). Compared E-plane pattern between initial uniform conformal array (SLL=-17.3dB) and sparse array (SLL=-27.8dB) is given in Fig. 8 (c). The PSLL of optimized sparse conformal array is far less than that of the initial uniform one. The proposed method can be also combined with the optimization of element excitations, not only positions, to realize lower SLL.
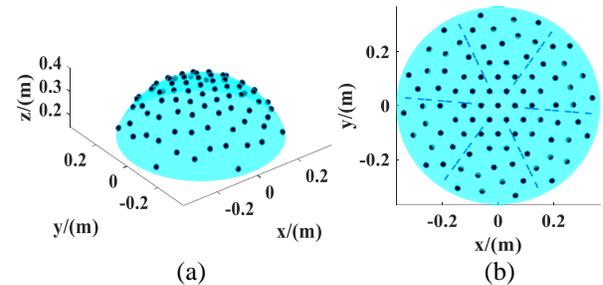

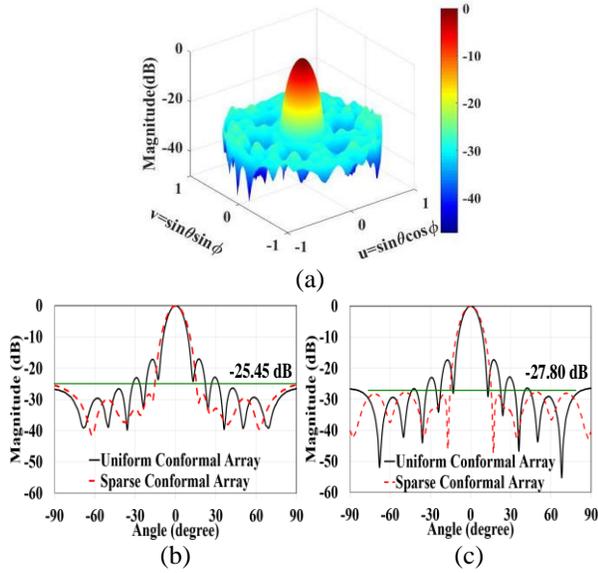Fig. 7. (a) Sparse hemisphere array. (b) Planform of sparse hemisphere array.

(a)

(b)

(c)

Fig. 8. (a) Optimized pattern. (b) Cut pattern φ=26˚ of sparse hemisphere array. (c) E-plane pattern of sparse hemisphere array.

Moreover, we vary the sector number Q to discuss relevant influences on the performance of synthesized patterns for sparse conformal array. The same array configuration is used. Though, the number of optimized sparse array remains nearly constant, different Q brings about different optimizable element number for one sector. Detailed performances of conformal synthesized patterns with different sectors are shown in Table 1, where the PSLL, and total number N are given. It is interesting to note that different sector numbers cause different effects on the radiation property of sparse conformal array. Though more sectors directly reduce the optimizing dimension of conformal array, but it is not linearly related to the better radiation performance. The top view of sparse conformal array element distribution with rotational sectors of Q=5 and Q=8 is respectively shown in Figs. 9 (a) and (b). The 3D pattern of optimized sparse conformal array with Q=8 is shown in Fig. 10 (a). E-plane pattern and cut-plane (φ=138˚) pattern of synthesized sparse conformal array is compared with uniform conformal array in Fig. 10 (b), where the PSLL is marked with green line as -26.53 dB in φ=138˚.

Table1: Investigation of rotational sector number

Sector Number Q	Element Number of Each Sector	Total Number N'	PSLL (dB)
5	18	91	−24.46
6	15	91	−25.45
7	13	92	−24.25
8	11	89	−26.53
9	10	91	−26.41

(a)

(b)
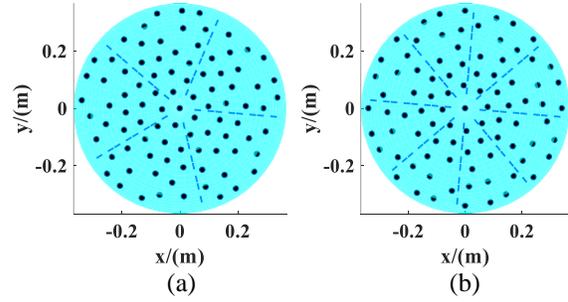
Fig. 9. (a) Element distribution with Q=5. (b) Element distribution with Q=8.

(a)

(b)
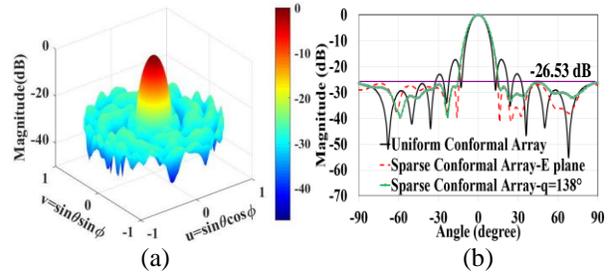
Fig. 10. (a) Optimized pattern. (b) Cut pattern φ=138˚ and E-plane pattern of sparse hemisphere array.

Table 2: Investigation of sparse ratio

Total Number N'	Sparse Ratio γ (%)	PSLL (dB)
55	53.4	−27.09
67	43.2	−28.34
73	38.1	−29.91
91	23	−26.60

To further verify the influence of different sparse ratios γ on the performance of synthesized sparse conformal pattern, the array number varies from 55 to 91 with the same initial conformal array geometry of the first numerical example. The rotational sector Q is fixed as 6. The radiation behaviors of synthesized sparse array with different sectors are shown in Table 2, where PSLL, sparse ratio γ and total number N are listed. Though the sparse conformal array allows to have more freedom of element distributions to improve array performance, but not the less element number the better radiation behavior. The optimized sparse conformal array (N'=73) has the best performance of SLL=-29.91dB with sparse ratio of 38.1%, where its E-plane pattern and top view of element layout is respectively shown in Figs. 11 (a) and (b). Then, with the increasing of reduced elements, the radiation behavior of SLL will be raised from -29.91dB to -27.09dB. The E-plane and H-plane pattern of the conformal sparse array ($N'=55$) is presented in Figs. 12 (a) and (b) respectively, its corresponding top view of element distribution is shown in Fig. 12 (c).
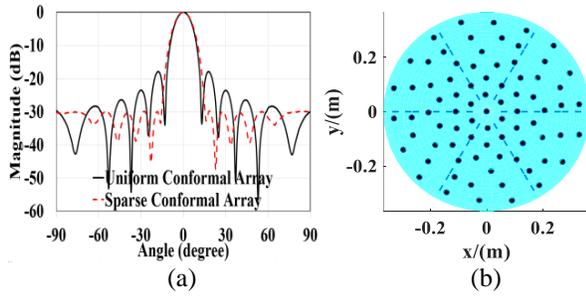
(a)   (b)

Fig. 11. (a) Synthesized E-plane pattern of sparse hemisphere array. (b) Element distribution with N=73.

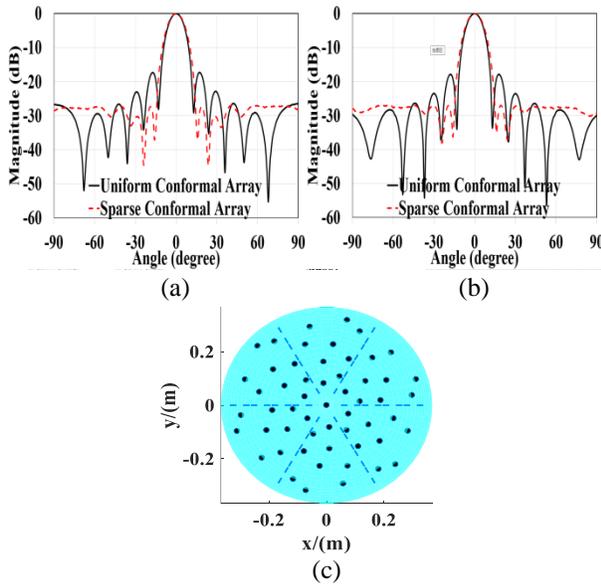(a)   (b)

(c)

Fig. 12. (a) Synthesized pattern of E-plane for sparse hemisphere array. (b) Synthesized pattern of H-plane for sparse hemisphere array. (c) Element layout with N=55.

Moreover, the comparison behaviors of synthesized patterns with other presented approaches of NSGAII [11] and PSOGA [14] are compared in Table 3. The proposed method has better performance of lower SLL in different sparse ratio conditions compared with the synthesized results optimized by NSGAII and PSOGA.

Table 3: Comparison between SLL of the hemisphere array with different sparse ratio

Number N'	Sparse Ratio γ (%)	NSGAII [11]	PSOGSA [14]
55	53.4	-20.1	-24.8
67	43.2	-20.4	-25.1
73	38.1	-21.1	-25.5
91	23.0	-21.6	-26.1

Moreover, the proposed method is further exploited to the synthesis of sparse conformal arrays in wide angle

scanning. For the initial $\lambda/2$ uniform spacing conformal array, the equivalent antenna number on the hemisphere surface is 265 with nine circular subarrays; see Fig. 13. The radius of the hemisphere is 6λ corresponding to the free wavelength at 2.45GHz. All elements are initially given uniform excitations.

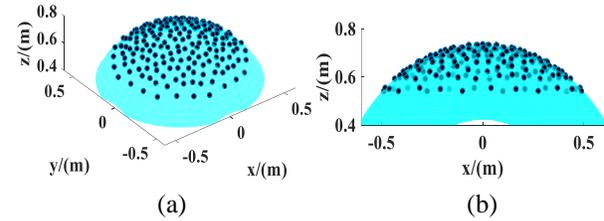(a)   (b)

Fig. 13. (a) Uniform hemisphere array. (b) Left view of uniform hemisphere array.

The optimized design of sparse conformal array is selected to divide into 8 symmetric conformal regions with N_Q elements and $2N_Q$ optimizable variables per part. The topmost unit remains motionless. The elements in the fold are limited to the region defined by ($r_q = 3\lambda$, $0 \leq \phi_q \leq 2\pi/6$, $0 \leq \theta_q \leq \pi/2$). The scanning angle θ covers from 0° to 60° with 15°−uniform space and φ is fixed to be 0°. The desired SLL is set to be -20dB. Firstly, the optimizable excitations of sparse conformal elements all set to be one. The sparse array reaches the SLL of -20.0dB with a minimum element spacing of 0.51λ within the scanning angle from 0° to 45° upon 500 iterative optimizing steps, but the SLL of the synthesized sparse conformal array is −18.19 dB in the larger scanning angle of 60°. The total element number of optimized array is 185. The sparse ratio γ is 30.2%. The optimization requires nearly 1.18 hour.

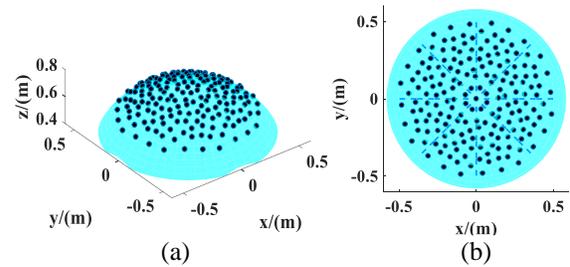(a)   (b)

Fig. 14. (a) Sparse hemisphere array. (b) Top view of sparse conformal hemisphere array.

The optimized conformal sparse element locations are shown in Fig. 14 (a) and its top view is given in Fig. 14 (b). The synthesized sparse conformal patterns of equal excitations in different scanning angle are compared with the patterns of initial uniform array in Fig. 15. The black lines are the main cut pattern of uniform array in different

angle scanning and the lines with the cross symbol represent main cut pattern of sparse conformal array in different angle scanning.
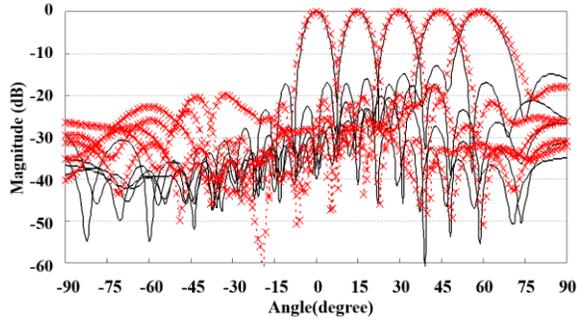

Fig. 15. Comparison of synthesized sparse conformal patterns of equal excitations with the initial uniform conformal array.

To further reduce the sidelobe level, the amplitude excitations of sparse conformal array elements are exploited into the optimizing procedure of the rotational symmetry BSO method. The synthesized sparse conformal patterns of optimized excitations in different angle scanning are presented in Fig. 16. The synthesized results of uniform array with equal excitations, sparse conformal array with equal excitations and optimized excitations are detailed-compared in Table 4. It can be seen that the sparse conformal array with the further optimization of excitations have better performance of the SLL under -25dB in wide angle scanning.
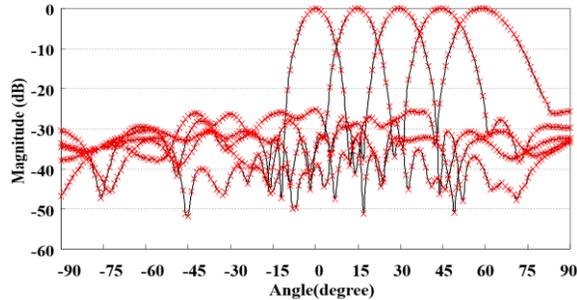

Fig. 16. Synthesized sparse conformal patterns of optimized excitations.

Table 4: Comparison between SLL of the hemisphere array in wide angle scanning

Scanning Angle (θ, ϕ)	Uniform Array (dB)	Sparse Array1 (dB)	Sparse Array2 (dB)
(0°, 0°)	-17.24	-22.15	-32.04
(15°, 0°)	-17.56	-21.46	-30.96
(30°, 0°)	-16.05	-20.64	-30.21
(45°, 0°)	-14.81	-20.05	-27.71
(60°, 0°)	-12.84	-18.19	-25.67

Moreover, we vary the d_{target} to investigate the relationship between sparse ratio and sparse conformal array performance in wide-angle scanning. The d_{target} varies from 0.45λ to 0.7λ. The minimum element space constraint of d_{target} directly influences the sparse ratio of reconstructed array when fixed aperture. The larger the element space, the higher the sparse ratio. Detailed radiation performance varying d_{target} is shown in Table 5. It is not entirely true that the more elements, the better the radiation behavior such as d_{target}=0.45λ and d_{target}=0.5λ. However, smaller spacing and more elements may make it easier to achieve lower SLL in larger scanning angle, e.g., 60°. With the further increase of d_{target} from 0.5λ to 0.7λ, the sparse ratio rises to 42.3%. But, the SLL behavior is getting worse especially in larger scanning angle, whose SLL is only -13.76dB in (60°, 0°)-scanning angle with d_{target}=0.7λ. The sparse array distribution with d_{target}=0.7λ and its top view is shown in Figs. 17 (a) and (b). The synthesized pattern of sparse array in different angle scanning is shown in Fig. 18 (a) and its 3D pattern in 0° and 60° is presented in Figs. 18 (b) and (c), respectively.

Table 5: SLL comparison of sparse array varying d_{target} in wide angle scanning

d_{target} (λ)	0.45	0.5	0.6	0.7
Sparse Ratio γ (%)	24.1	30.2	36.2	42.3
(0°, 0°)	-21.36	-22.15	-21.02	-19.39
(15°, 0°)	-20.87	-21.46	-20.31	-18.77
(30°, 0°)	-20.16	-20.64	-19.24	-16.56
(45°, 0°)	-19.78	-20.05	-18.48	-14.98
(60°, 0°)	-18.96	-18.19	-17.25	-13.76

(a)   (b)
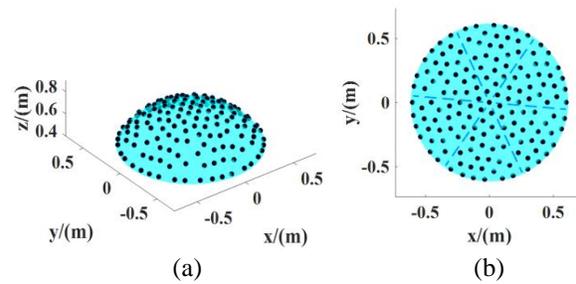
Fig. 17. (a) Sparse conformal array of d_{target}=0.7λ. (b) Top view of reconstructed sparse conformal array.

With the synthesized sparse conformal array distribution Fig. 14 of above multiple-pattern optimizing numerical example, the reference flat-top pattern of [9] is formed as the desired objective to be optimized and designed by the proposed method. The SLL within the coverage of $\theta \in [-90°, -30°]$ and $[30°, 90°]$ is set as

-30dB, the normalized Gain of synthesized conformal pattern fluctuates no more than 1dB up or down in the coverage angle of $\theta \in [-15°, 15°]$. The synthesized flat-top pattern of sparse conformal array is presented in Fig. 19 with 400 iterative optimizing steps. The optimized *SLL* in the designated region is -29.83 dB, which is close to the expected value of -30dB. The performance of the designed pattern in the fluctuant zone also meets the desired requirement, which is in the range of ± 0.95dB.
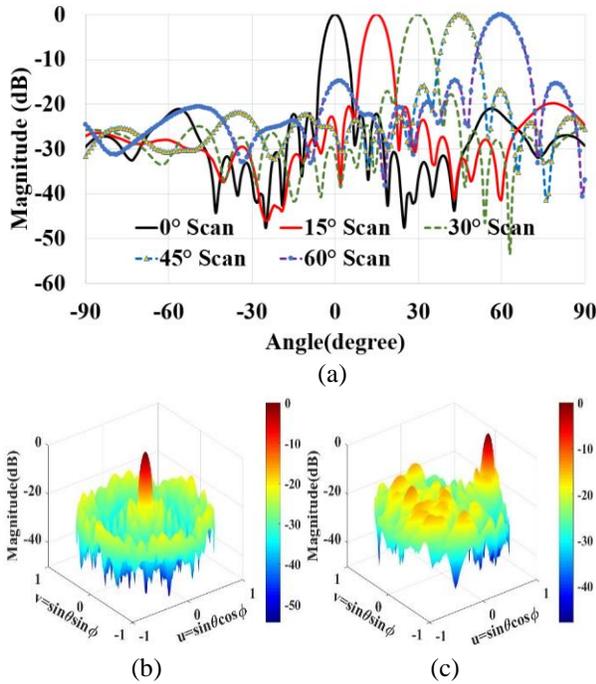

(a)

(b)   (c)

Fig. 18. (a) synthesized pattern of different scanning angle under d_{target}=0.7λ. (b) 3D pattern of direction 0°. (c) 3D pattern of direction 60°.
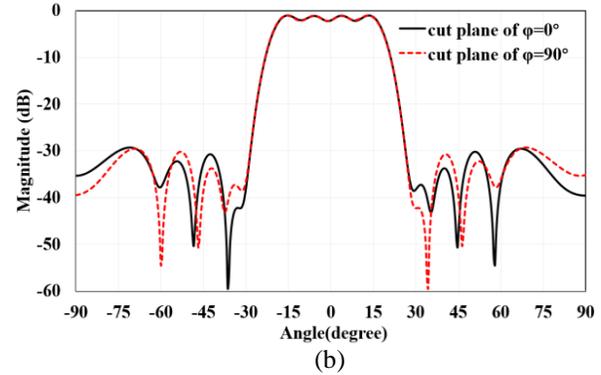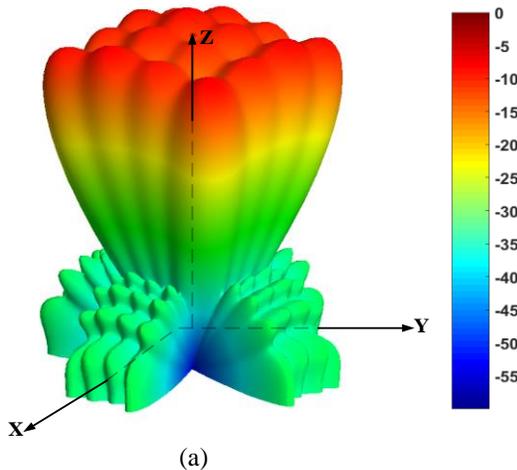

(a)

(b)

Fig. 19. Synthesized shaped-beam pattern of sparse conformal array: (a) 3D view of flat-top pattern; (b) different cut plane patterns.

IV. CONCLUSION

A novel hybrid rotationally symmetric sparse conformal array design techniques is introduced in the paper to find the solutions under multiple constraints. Exploiting rotational symmetry not only provides a way to simplify optimal designs, but also accelerate the optimization of larger conformal arrays in the same computing resources. The problem size is reduced by only optimizing element distributions in a small conformal slice of the carrier surface aperture. Numerical results indicate that the proposed method can design sparse conformal arrays with lower sidelobe levels and suppresses grating lobes in wide angle scanning. In addition, we investigate the effects of sparse ratio on synthesized patterns. Further works will take account of the mutual coupling effects on actual conformal array elements into the synthesis and optimizing procedure of large sparse conformal arrays.

ACKNOWLEDGMENT

REFERENCES

[1] K. Chen, Z. S. He, and C. L. Han, "A modified real GA for the sparse linear array synthesis with multiple constraints," *IEEE Trans. Antennas Propag.*, vol. 54, no. 7, pp. 2169-2173, July 2006.

[2] K. Chen, X. Yun, Z. He, and C. Han, "Synthesis of sparse planar arrays using modified real genetic algorithm," *IEEE Trans. Antennas Propag.*, vol. 55, no. 4, pp. 1067-1073, Apr. 2007.

[3] S. K. Goudos, K. Siakavara, T. Samaras, Elias E. Vafiadis, and J. N. Sahalos, "Sparse linear array

synthesis with multiple constraints using differential evolution with strategy adaptation," *IEEE Antennas Wireless Propag. Lett.*, vol. 10, pp. 670-673, July 2011.

[4] H. Liu, H. W. Zhao, W. M. Li, and B. Liu, "Synthesis of sparse planar arrays using matrix mapping and differential evolution," *IEEE Antennas Wireless Propag. Lett.*, vol. 15, pp. 1905-1908, Mar. 2016.

[5] K. V. Deligkaris, Z. D. Zaharis, D. G. Kampitaki, S. K. Goudos, I. T.Rekanos, and M. N. Spasos, "Thinned planar array design using Boolean PSO with velocity mutation," *IEEE Trans. Mag.*, vol. 45, no. 3, pp. 1490-1493, Mar. 2009.

[6] G. Oliveri, M. Carlin, and A. Massa, "Complex-weight sparse linear array synthesis by Bayesian compressive sampling," *IEEE Trans. Antennas Propag.*, vol. 60, no. 5, pp. 2309-2325, May 2012.

[7] G. Oliveri and A. Massa, "Bayesian compressive sampling for pattern synthesis with maximally sparse non-uniform linear arrays," *IEEE Trans. Antennas Propag.*, vol. 59, no. 2, pp. 467-481, Feb. 2011.

[8] Y. H. Liu, Q. H. Liu, and Z. P. Nie, "Reducing the number of elements in multiple-pattern linear arrays by the extended matrix pencil methods," *IEEE Trans. Antennas Propag.*, vol. 62, no. 2, pp. 652-660, Feb. 2014.

[9] P. F. Gu, G. Wang, Z. H. Fan, and R. S. Chen, "Efficient unitary matrix pencil method for synthesising wideband frequency patterns of sparse linear arrays," *IET Microwaves Antennas and Propagation*, vol. 12, pp. 1871-1876, May 2018.

[10] P. F. Gu, G. Wang, Z. H. Fan, and R. S. Chen, "An efficient approach for the synthesis of large sparse planar array," *IEEE Transactions on Antennas and Propagation*, vol. 67, no. 12, pp. 7320-7330, Aug. 2019.

[11] J. O. Yang, Q. R. Yuan, F. Yang, H. J. Zhou, and Z. P. Nie, "Synthesis of conformal phased array with improved NSGA-II algorithm," *IEEE Trans. Antennas Propag.*, vol. 57, no. 12, pp. 4006-4009, June 2009.

[12] M. A. N. Fakher, "Pattern synthesis for a conformal array antenna mounted on a paraboloid reflector using genetic algorithms," *Applied Computational Electromagnetics Society Journal*, vol. 30, no. 2, pp. 230-236, Feb. 2015.

[13] Y. Y. Bai, S. Xiao, C. Liu, and B. Z. Wang, "A hybrid IWO/PSO algorithm for pattern synthesis of conformal phased arrays," *IEEE Trans. Antennas Propag.*, vol. 61, no. 4, pp. 2328-2332, Apr. 2012.

[14] B. Sun, C. Liu, Y. Liu, X. Wu, Y. Li, and X. Wang, "Conformal array pattern synthesis and activated elements selection strategy based on PSOGSA

algorithm," *Int. J. Antennas Propag.*, vol. 6, pp. 1-11, June 2015.

[15] H. L. Li, Y. C. Jiang, Y. Ding, J. Tian, and J. J. Zhou, "Low-sidelobe pattern synthesis for sparse conformal arrays based on PSO-SOCP optimization," *IEEE Access*, vol. 6, pp. 77429-77439, Nov. 2018.

[16] J. L. Guo and J. Y. Li, "Pattern synthesis of conformal array antenna in the presence of platform using differential evolution algorithm," *IEEE Trans Antennas Propag.*, vol. 57, no. 9, pp. 2615-2621, Sep. 2009.

[17] T. K. Vo Dai, T. Nguyen, and O. Kilic, "A non-focal Rotman lens design to support cylindrically conformal array antenna," *Applied Computational Electromagnetics Society Journal*, vol. 33, no. 2, pp. 240-243, Feb. 2018.

[18] Z. Li, L. Tan, X. Kang, J. Su, Q. Guo, Y. Yang, and J. Wang, "A novel wideband end-fire conformal antenna array mounted on a dielectric cone," *Applied Computational Electromagnetics Society Journal*, vol. 31, no. 8, pp. 959-966, Aug. 2016.

[19] Y. Shi, "Brain storm optimization algorithm," in *Advances in Swarm Intelligence*, Y. Tan, Y. Shi, Y. Chai, and G. Wang, Eds., Berlin, Heidelberg: Springer Berlin Heidelberg, pp. 303-309, 2011.

[20] C. Sun, H. Duan, and Y. Shi, "Optimal satellite formation reconfiguration based on closed-loop brain storm optimization," *IEEE Computational Intelligence Magazine*, vol. 8, no. 4, pp. 39-51, Nov. 2013.

[21] Z. Xu, X. F. Li, X. T. Meng, and Y. T. Liu, "A distributed brain storm optimization for numerical optimization and graph planarization," *IEEE Access*, vol. 7, pp. 39770-39781, Apr. 2019.

[22] Y. X. Jiang, X. Chen, F. C. Zheng, T. D. Niyato, and X. H. You, "Brain storm optimization-based edge caching in fog radio access networks," *IEEE Transactions on Vehicular Technology*, 2021, early access.

[23] A. Aldhafeeri and Y. R. Samii, "Brain storm optimization for electromagnetic applications: Continuous and discrete," *IEEE Trans. Antennas Propag.*, vol. 67, no. 40, pp. 2710-2722, Jan. 2019.

[24] V. Pierro, V. Galdi, G. Castaldi, I. M. Pinto, and L. B. Felsen, "Radiation properties of planar antenna arrays based on certain categories of aperiodic tilings," *IEEE Trans. Antennas Propag.*, vol. 53, no. 2, pp. 635-644, Feb. 2005.

[25] A. F. Morabito and P. G. Nicolaci, "Optimal synthesis of shaped beams through concentric ring isophoric sparse arrays," *IEEE Antennas Wireless Propag. Lett.*, vol. 16, pp. 979-982, Apr. 2017.

[26] M. D. Gregory, F. A. Namin, and D. H. Werner, "Exploiting rotational symmetry for the design of ultra-wideband planar phased array layouts," *IEEE*

Trans. Antennas Propag., vol. 61, no. 1, pp. 176-184, Jan. 2013.

Pengfei Gu was born in Nanjing, China. He received the B.S. and Ph.D. degrees in Electromagnetic Field and Microwave Technique from the School of Electrical Engineering and Optical Technique, Nanjing University of Science and Technology, Nanjing, China, in 2012 and 2019 respectively. He is currently pursuing post-doctoral in Electronic and Communication Engineering at Nanjing University of Science and Technology. His research interests are antennas, array optimizations, array sparse and computational electromagnetics.

Zhenhong Fan was born in Jiangsu, China, in 1978. He received the M.Sc. and Ph.D. degrees in Electromagnetic Field and Microwave Technique from the Nanjing University of Science and Technology (NJUST), Nanjing, China, in 2003 and 2007, respectively. In 2006, he was a Research Assistant with the Center of wireless Communication, City University of Hong Kong. He is currently a Professor of Electronic Engineering with NJUST. He is the author or a coauthor of over 50 technical articles. His current research interests include computational electromagnetics, and electromagnetic scattering and radiation.

Dazhi Ding received the B.Sc. and Ph.D. degrees in Electromagnetic Field and Microwave Technique from Nanjing University of Science and Technology (NJUST), Nanjing, China, in 2002 and 2007, respectively. During 2005, he was with the Center of wireless Communication in the City University of Hong Kong, Kowloon, as a Research Assistant. He joined the Department of Electrical Engineering, Nanjing University of Science and Technology (NJUST), Nanjing, China, where he became a Lecturer in 2007. In 2014, he was promoted to Full Professor in NJUST. He was appointed Head of the Department of Communication Engineering, NJUST in September 2014. He is the author or coauthor of over 30 technical papers. His current research interests include computational electromagnetics, electromagnetic scattering and radiation. He has authored or coauthored more than 80 papers. He is the recipient of the Foundation for China Excellent Young Investigators presented by the National Science Foundation (NSF) of China in 2015.

Rushan Chen received the B.Sc. and M.Sc. degrees from the Department of Radio Engineering, Southeast University, China, in 1987 and 1990, respectively, and the Ph.D. degree from the Department of Electronic Engineering, City University of Hong Kong, in 2001.

He joined the Department of Electrical Engineering, Nanjing University of Science and Technology (NJUST), China, where he became a Teaching Assistant in 1990 and a Lecturer in 1992. Since September 1996, he has been a Visiting Scholar with the Department of Electronic Engineering, City University of Hong Kong, first as Research Associate, then as a Senior Research Associate in July 1997, a Research Fellow in April 1998, and a Senior Research Fellow in 1999. From June to September 1999, he was also a Visiting Scholar at Montreal University, Canada. In September 1999, he was promoted to Full Professor and Associate Director of the Microwave and Communication Research Center in NJUST, and in 2007, he was appointed as the Head of the Department of Communication Engineering, NJUST. He was appointed as the Dean in the School of Communication and Information Engineering, Nanjing Post and Communications University in 2009. And in 2011 he was appointed as Vice Dean of the School of Electrical Engineering and Optical Technique, NJUST. Currently, he is a principal investigator of more than 10 national projects. His research interests mainly include computational electromagnetics, microwave integrated circuit and nonlinear theory, smart antenna in communications and radar engineering, microwave material and measurement, RF-integrated circuits, etc. He has authored or coauthored more than 260 papers, including over 180 papers in international journals.